POLITECNICO DI TORINO

MSc Automotive Engineering

A.Y. 2023/24

Aerodynamics laboratory report

Carlo Vittorio Colucci 329703

January 15, 2024

Contents

1 1st laboratory **1**

1.1 Mesh setup and generation 1

1.2 Simulation setup and run 4

1.3 Analysis of results 4

2 2nd laboratory **10**

2.1 Post-processing 10

2.2 Comparative analysis of results 12

1 1st laboratory

The goal of this project is to evaluate the aerodynamic performance of an Alfa Romeo MiTo by means of CFD tools.

1.1 Mesh setup and generation

The choice of the mesh size is a crucial step during the aerodynamic analysis of a vehicle. Indeed, the quality of the results is strictly dependent on this parameter, as well as the simulation computational time. Thus the designer's duty is to reach an optimal trade-off between these two aspects.
The base mesh size adopted for this simulation is 25mm, but refinement regions are set up to increase results accuracy where needed, for instance where the air flow detaches from the vehicle surface. Both surface and volume meshes are tuned. The most relevant parameter in this step is the target size, expressed in percentage with respect to the base size.
Starting from the surface meshes, the following regions are affected with the relative parameters:

Region	**Target size [%]**
All vehicle	200
Aero-surfaces	75
Tunnel floor	2500
Tunnel exterior	5000

Table 1: Surface mesh

For ease of interpretation the involved regions are depicted as well:

Figure 1: All vehicle

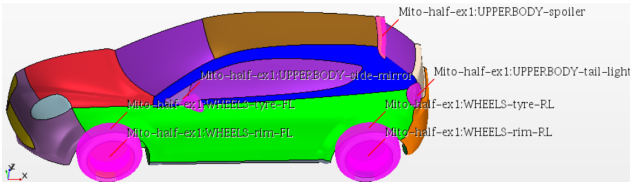

Figure 2: Aero-components

Figure 3: Tunnel floor

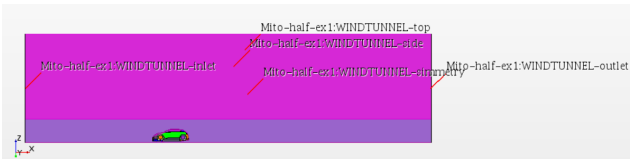

Figure 4: Tunnel exterior

Going on with the volume meshes:

Region	**Target size [%]**
Vehicle components	75
Vehicle wake	200
Vehicle 1	500
Vehicle 2	1000

Table 2: Volume mesh

In this cases the involved regions are depicted too:

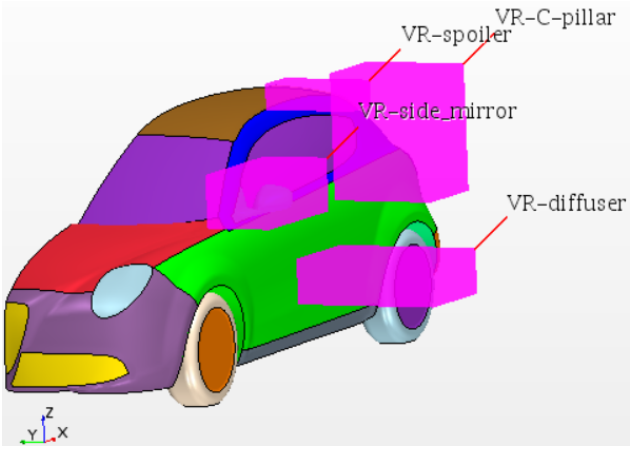

Figure 5: Vehicle components

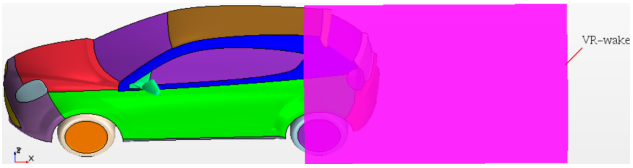

Figure 6: Vehicle wake

Figure 7: Vehicle 1

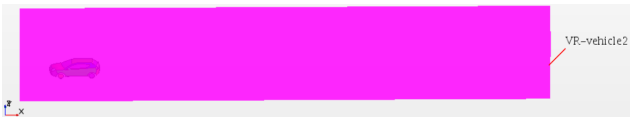

Figure 8: Vehicle 2

After that the mesh parameters are properly set up for the different regions within the simulation environment, the volume mesh is generated with a global number of cells equal to 404465. It's also possible to implement plane sections to check whether the resulting mesh is as expected: all the refinement regions should present a different mesh texture with respect to the basic one. The graphical result follows:

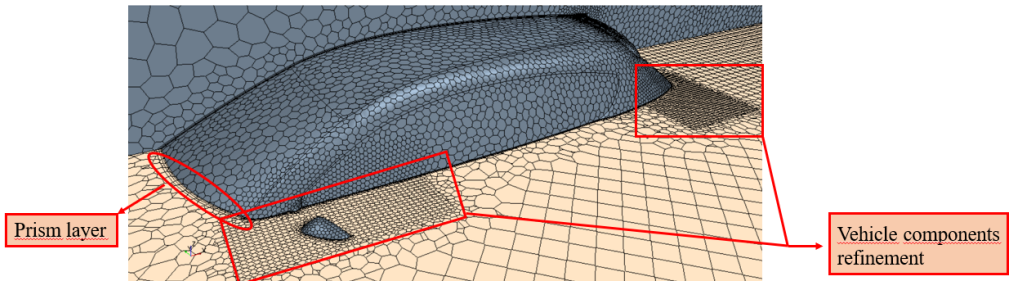

Figure 9: Mesh check of the simulation system

As highlighted the prism layer is successfully obtained, as well as the refinement regions.

1.2 Simulation setup and run

Once the discretized model is retrieved, the last fundamental step, before to run the simulation and so to retrieve results, is to set up the physics behind the test to be simulated.
The air flow conditions, within the simulated wind tunnel, are:

- Density: $1.225\,kg/m^3$;
- Dynamic viscosity: $1.79e-5\,Pa\cdot s$;
- Initial uniform flow conditions: $\vec{v} = [20.0,\ 0.0,\ 0.0]\,m/s$;
- Wind tunnel inlet velocity: $38.89\,m/s$;
- Wind tunnel outlet pressure: $0\,Pa$.

The turbulence model adopted is the K-epsilon. Slip conditions are set for the wind tunnel front floor, simmetry plane and top and side faces.
With all the simulation parameters properly tuned, it's possible to run the simulation and to analyse the desired results.

1.3 Analysis of results

The first relevant parameter for aerodynamic applications is the vehicle frontal area which is equal to $1.036\,m^2$.
The other main parameters that the simulation returns are the Cx (drag) and Cz (lift) coefficients, that are important indicators of the aerodynamic performance and efficiency of the vehicle, independently of its weight. An analysis of how these coefficients vary their magnitude at different iterations during the simulation phase is shown in these plots:

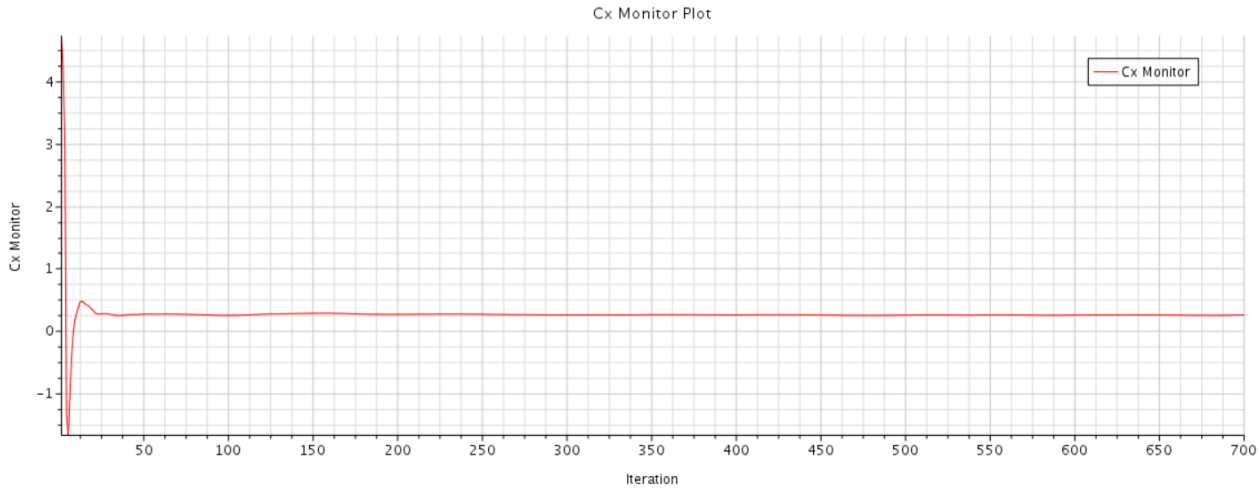

Figure 10: Cx monitor during the simulation phase

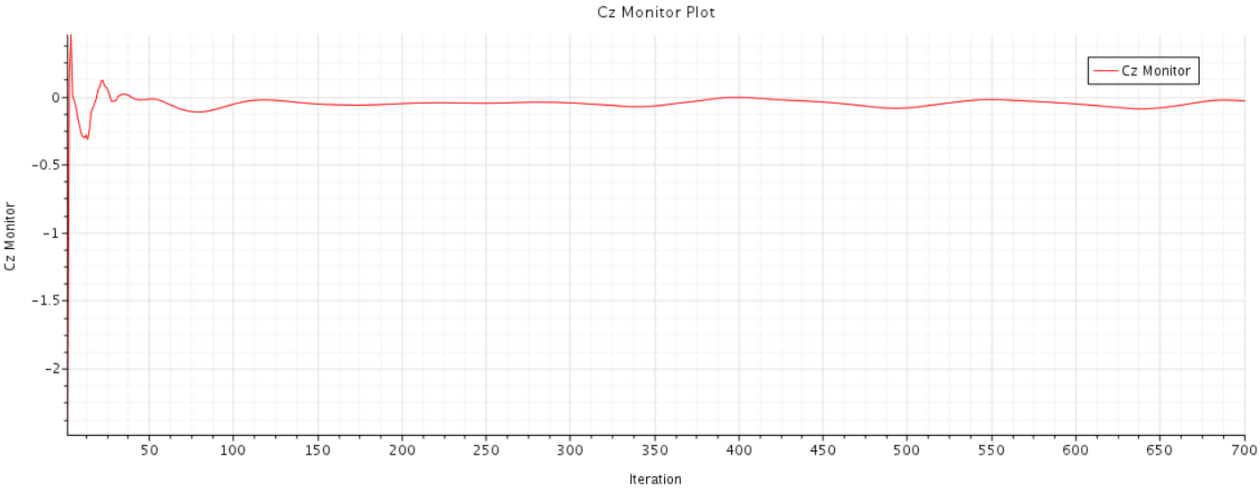

Figure 11: Cz monitor during the simulation phase

After a certain number of iterations, about 100, the coefficients value stabilises, attending very low fluctuations at much higher iterations number, standing for a good accuracy of the results, as highlighted in the residuals chart too:

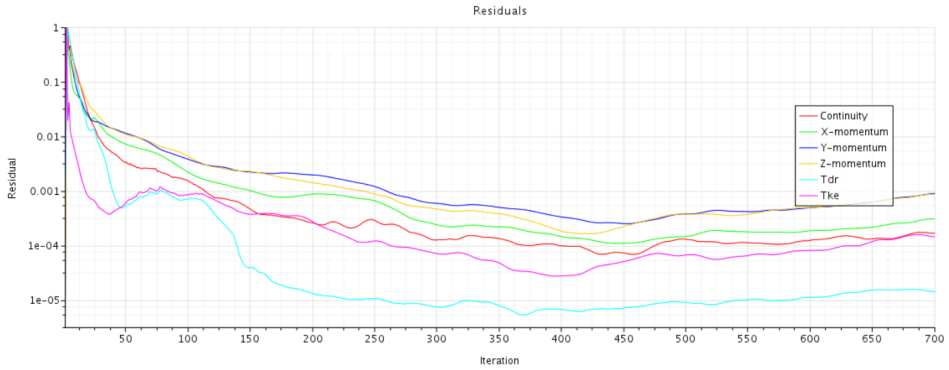

Figure 12: Residuals monitor during the simulation phase

In this chart is shown how accurate are the simulation results obtained through the utilization of the discretized equations. The results are good due to a low relative drop of the residuals: about 2 orders of magnitude. Also the steady values are enough small: lower than 10^{-3} (the ideal magnitude would be around the machine precision).
The final values of drag and lift coefficients obtained by the simulation follow:

- Cx = 0.258;
- Cz = -0.33.

These parameters are quite close to the experimental ones retrieved by the tests undertaken in the wind tunnel:

- Cx = 0.290;
- Cz = 0.1.

Discrepancies are always present, related to the implicit approximation of the methodologies adopted for the simulation.
Furthermore it's possible to analyse how the drag coefficient value evolves along the vehicle longitudinal direction:

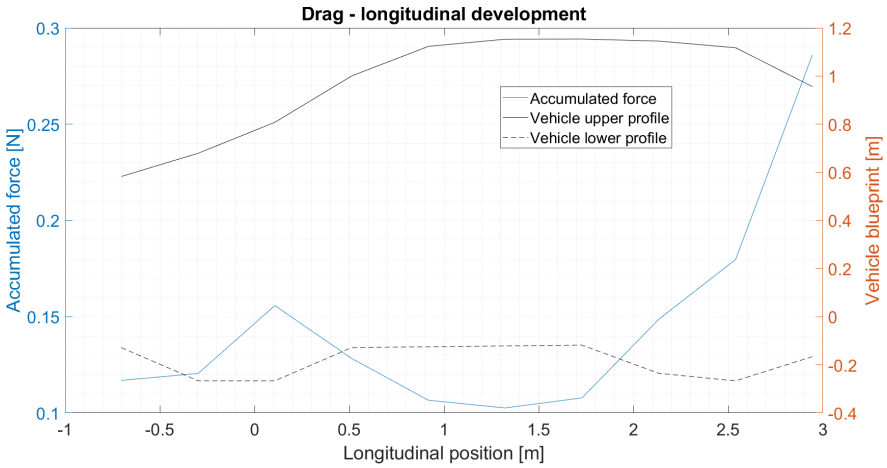

Figure 13: Drag - longitudinal development

To analyse the aerodynamic performance of the MiTo, it's necessary to view the distribution of the following parameters:

- pressure distribution on the vehicle surface;
- skin friction coefficient on the vehicle surface;
- velocity field around the vehicle;
- total pressure coefficient around the vehicle.

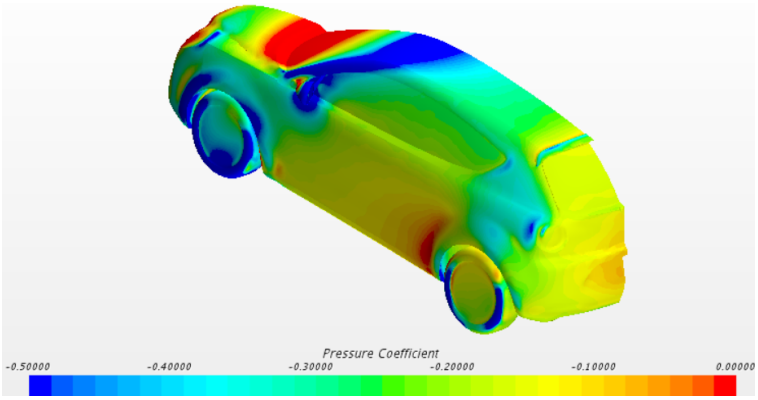

Figure 14: Pressure distribution on the vehicle surface

By means of this graphical representation it's possible to quickly recognise what are the regions where the vehicle attends a higher aerodynamic resistance, taking into account the pressure direction with respect to the vehicle one.
The vehicle front and the lower part of the windshield attend a high drag resistance.

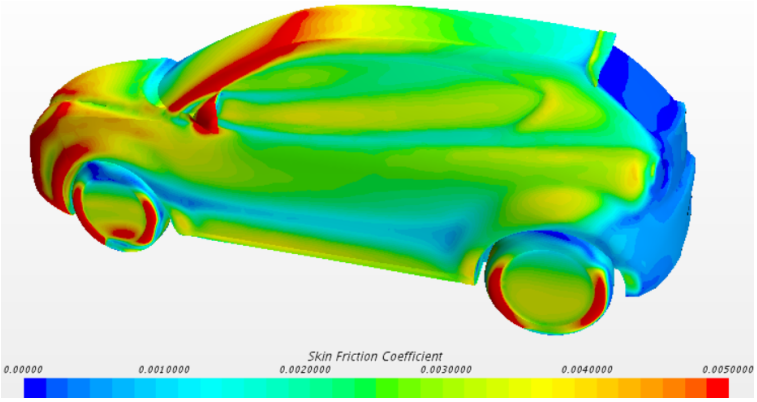

Figure 15: Skin friction coefficient on the vehicle surface

This coefficient is an important indicator of the flow behaviour: for positive values the flow is attached to the vehicle surface, getting separated for a none value, becoming a reverse-flow for negative values. In this case the flow gets detached mainly on the back of the vehicle and nearby the wheels.

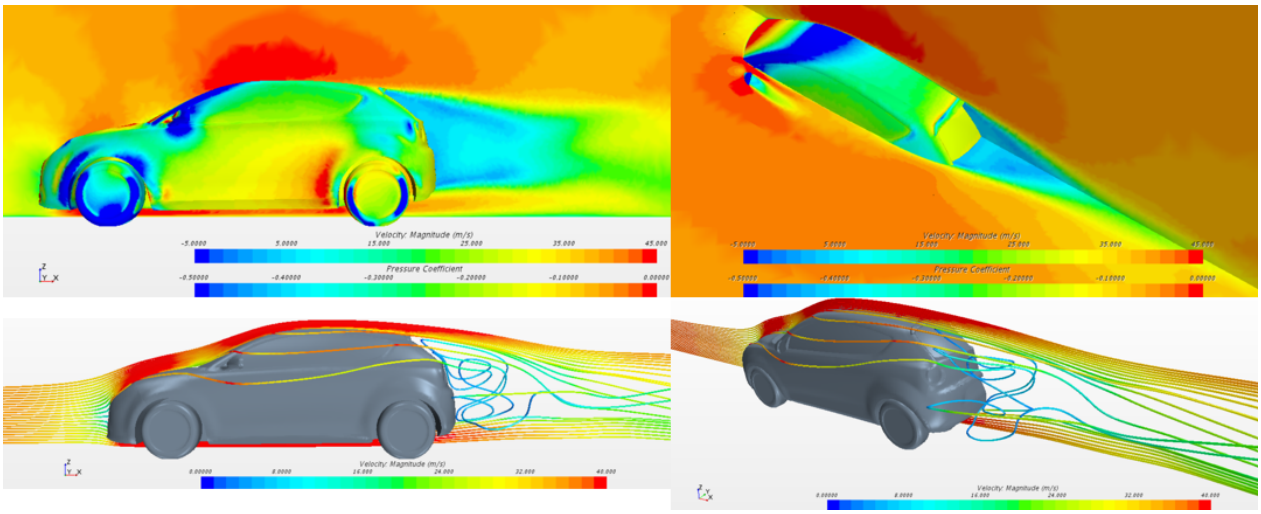

Figure 16: Velocity field around the vehicle

The air-flow is heavy perturbed behind the vehicle and nearby the side mirrors. In the streamline visualisation it's visible how the flow gets turbulent in the back and how it accelerates/decelerates along the vehicle.

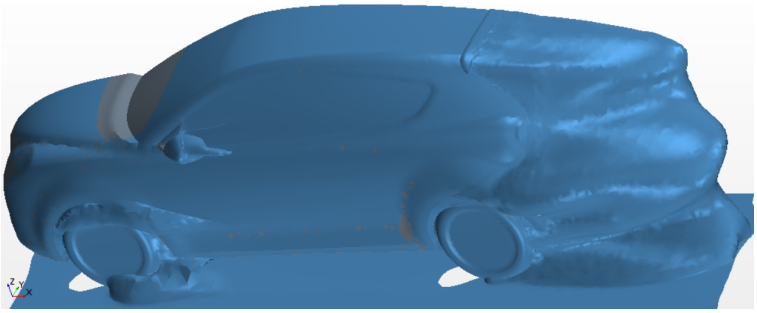

Figure 17: Total pressure coefficient around the vehicle

Through this representation the wake regions are highlighted, showing the aerodynamic impact on the air-flow of the different vehicle components.
The most turbulent region is on the back, as expected. This confirms the results previewed in Figure 16 and explains why the drag longitudinal development gets so high in this region, as shown in Figure 13.

2 2nd laboratory

The subject of this project is an Alfa romeo MiTo with rotating wheels. The goal is to compare two different geometric solutions for a vehicle component located opposite to the front wheels, analysing the impact on the overall vehicle aerodynamic performances.
The same simulation parameters of the previous laboratory are adopted to carry out the simulations.

2.1 Post-processing

In this section, for sake of simplicity, only the post-processing results relative to the vehicle with no spats are shown, while in the following section will be shown also the results relative to the other solution, but in a more specific way comparing them.
As in the previous laboratory, the distribution of the following parameters is shown:

- pressure distribution on the vehicle surface;
- skin friction coefficient on the vehicle surface;
- velocity field around the vehicle;
- total pressure coefficient around the vehicle.

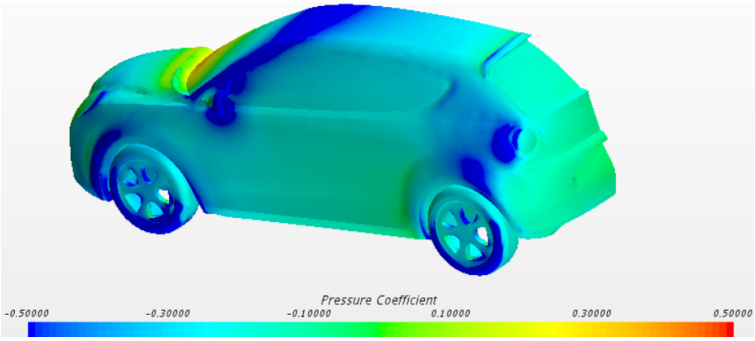

Figure 18: Pressure distribution on the vehicle surface

The pressure coefficient in the tailgate zone is close to 0, resulting in no drag generation. Instead, in the roof panel front region and in the bonnet region opposite to the front tire the pressure is slightly negative, standing for a drag recovery.

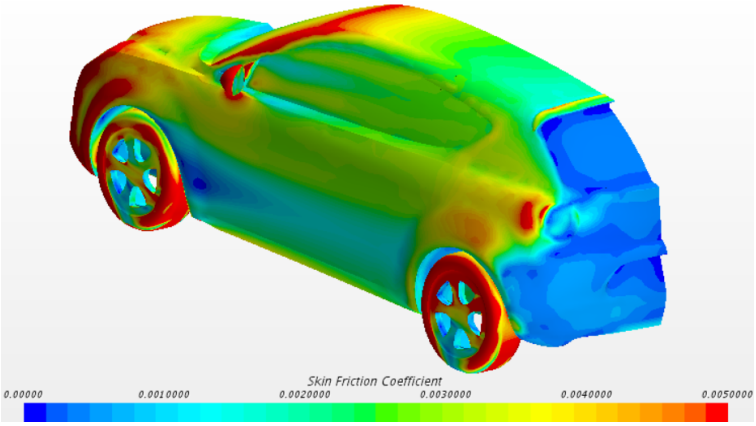

Figure 19: Skin friction coefficient on the vehicle surface

The flow detaches quite a lot aside of the vehicle behind of the front wheels, due to the perturbed flow generated by the rotating wheels. Behind the tailgate the flow completely detaches, apart of a small region close to the tail light, where the flow still keeps attached, leading to a performance worsening.

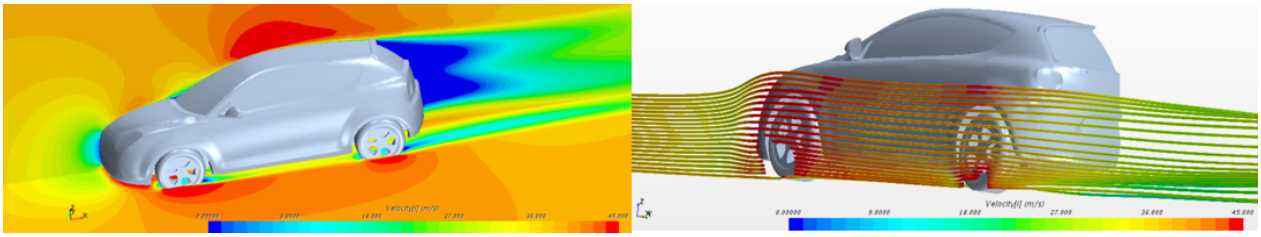

Figure 20: Velocity field around the vehicle

The flow is much accelerated aside of the vehicle, thus a wake region behind it is expected, the same holds for the regions behind the wheels, where the flow fields suddenly varies it's magnitude. The wakes evidence is shown in the following figure:

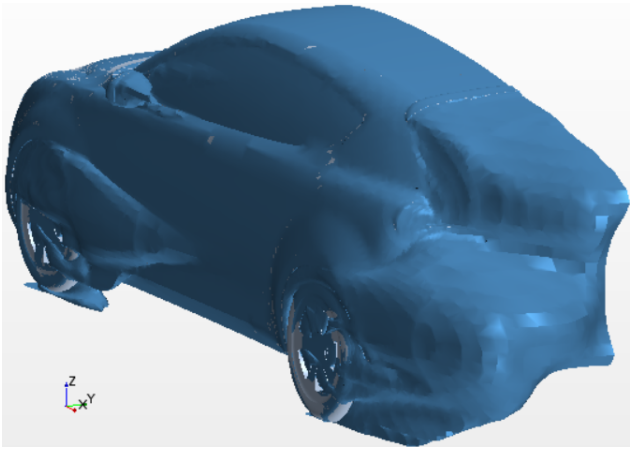

Figure 21: Total pressure coefficient around the vehicle

By means of this view the wake regions are highlighted, finding out a wide wake behind the vehicle, considerable wakes aside of the rotating wheels (wider than in the vehicle without rotating wheels) and smaller wakes behind the side mirrors.

2.2 Comparative analysis of results

The distribution of the main parameters useful for the analysis were presented, now the focus is on the comparison of the retrieved results for the two different geometrical solutions.

Starting from the vehicle frontal area the two values are:

- Vehicle with no spats: $S_{frontal} = 1.037\, m^2$;
- Vehicle with spats: $S_{frontal} = 1.045\, m^2$.

The vehicle with spats attends a slightly higher frontal area, that would lead to an increase in the resulting drag force on the vehicle.
The first aerodynamic parameters to be evaluated are the drag and lift coefficients of both the vehicles with the different embedded geometrical solutions:

- Vehicle with no spats: $C_x = 0.278, \quad Cz = -0.207$;
- Vehicle with spats: $C_x = 0.274, \quad Cz = -0.0528$.

Also a comparison of the drag trend along the vehicle longitudinal direction is shown:

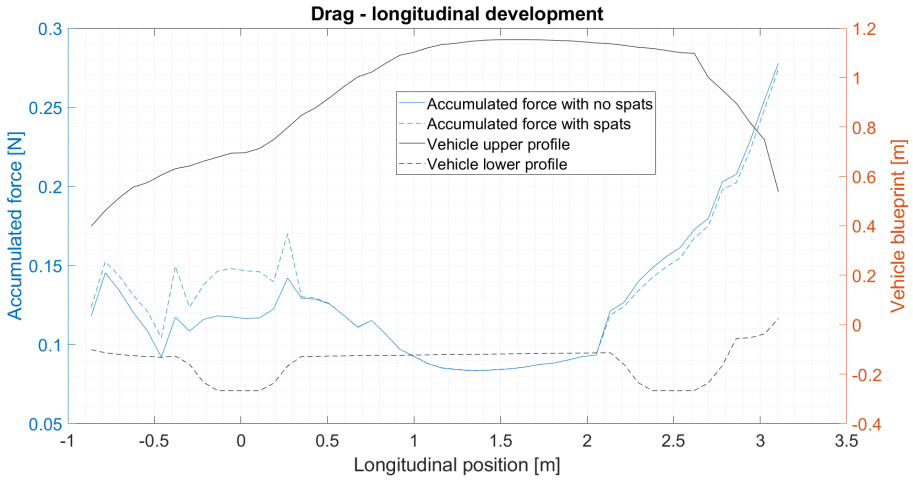

Figure 22: Drag - longitudinal development

The vehicle with spats, despite of an intensification of drag produced in the front wheels region, attends a reduction of drag in the rear wheels region, for reasons that are later clarified. The final drag coefficient value is lower, standing for an improvement in the aerodynamic efficiency. Quantifying the difference between the two geometrical solutions: $\Delta C_x = -0.004$. This value, retrieved by means of CFD simulations, is comparable with the one retrieved by wind tunnel tests, that is: $\Delta C_x = -0.006$. Once again the accuracy of the undertaken simulation is verified.

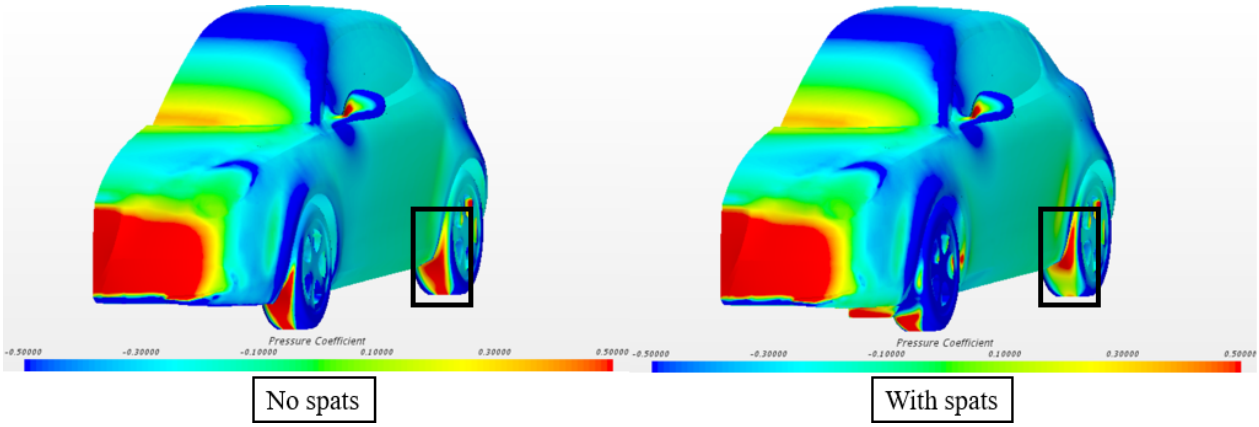

Figure 23: Comparison of the pressure distribution on the vehicle surface

In evidence of this aerodynamic improvement there is also the pressure distribution on the vehicle surface, in particular nearby the rear wheels, where the pressure magnitude is considerably minor.

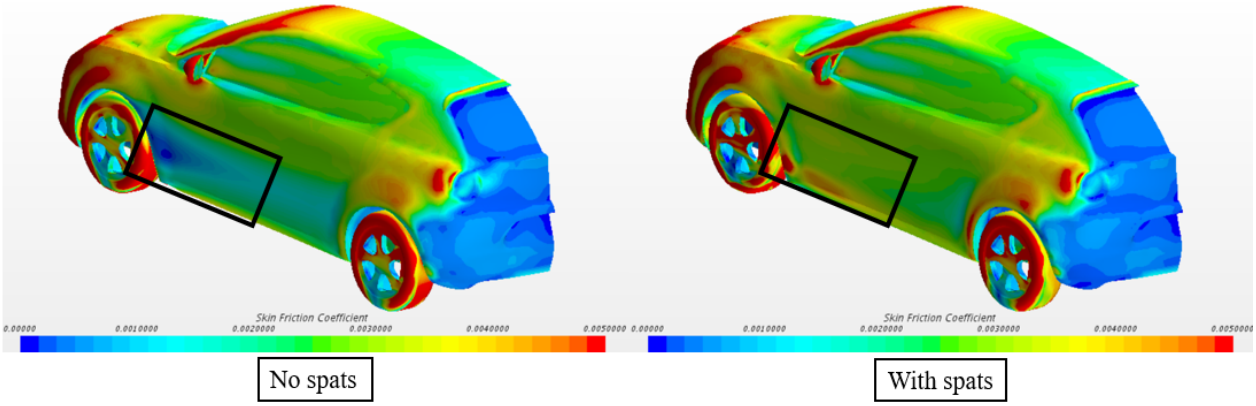

Figure 24: Comparison of the skin friction coefficient on the vehicle surface

Also the air flow keeps more attached to the vehicle surface. As highlighted in the figure, the flow on the vehicle front doors doesn't detach as it happens for the solution with no spats.

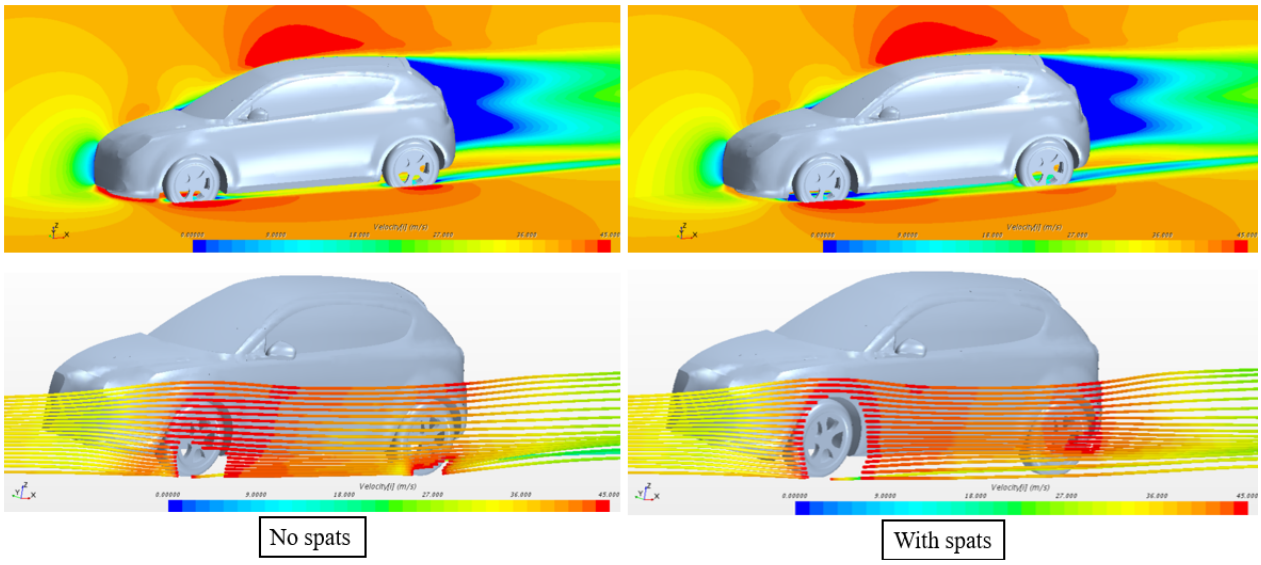

Figure 25: Comparison of the velocity field around the vehicle

The flow field leaving the rear wheels, behind the vehicle, is smoother for the geometrical solution with spats, as it's possible to view by the streamline visualization too. Also the flow under the vehicle nose is more distributed, resulting in an overall better flow distribution beneath the vehicle floor.

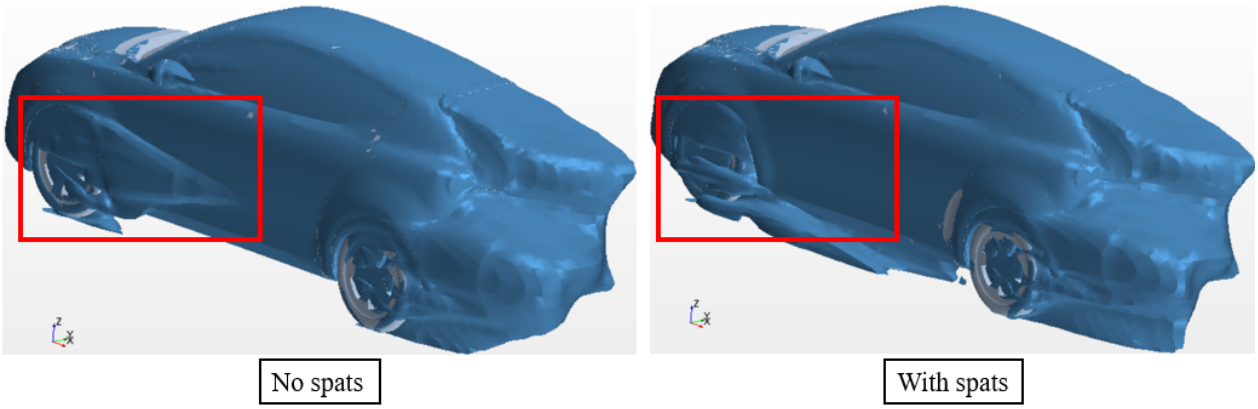

Figure 26: Comparison of the total pressure coefficient around the vehicle

Aside the front wheels the flow is less turbulent in the solution without spats, but it gets much more turbulent aside of the vehicle front door. This result is expected also considering the skin friction distribution evidenced in the Figure 24.

To conclude, the solution with spats is overall more aerodynamic efficient, due to a better flow guidance and wake regions control, counting for a $C_x \cdot A$ reduction of 2 counts. Thus the choice of this geometrical solution is optimal for the MiTo aerodynamic design.